

Large Deployable Antennas Benchmark for Contoured Beam Mission in C Band

Jakob Rosenkrantz de Lasson, Min Zhou, Cecilia Cappellin,
TICRA, Landemærket 29, DK-1119 Copenhagen K, Denmark, {jrdl,mz,cc}@ticra.com

Abstract—We report an RF benchmark study of large deployable antennas for a contoured beam mission in C band. With conventional solid shaped reflector antennas being limited to diameters of 3 m, we investigate solid shaped reflector antennas with aperture diameters of 3 m and 6 m as well as 6 m mesh reflector and reflectarray antennas. We consider a European coverage with directivity and XPD goals, and a realistic corrugated horn feed in a single-offset reflector configuration for the design of solid, mesh and reflectarray antennas. Our study shows that several 6 m mesh and reflectarray antennas perform better than the 3 m solid shaped antenna, which, upon further technological maturation, may pave the way for one or more of these novel antenna concepts in future contoured beam applications, when large (>3 m) apertures are required.

Index Terms—space, satellite application, contoured beam, reflector antenna, mesh reflector, reflectarray.

I. INTRODUCTION

Broadcasting signals to specific countries or continents on Earth from geostationary satellites is a billion-dollar business that, for example, provides TV and telephone coverage as well as data transmission. Delivering these signals only to limited regions on Earth relies on the generation of contoured beams, and since the early 1990s the standard for generating such beams has been shaped reflector antennas. An example of this concept for generating contoured beams for a European coverage can be seen in Fig. 1. One of the shaped reflectors can be inspected in Fig. 2, where “bumps” in the otherwise parabolic reflector surface produce the contoured beam.



Fig. 1. European (dashed magenta) and France and Germany (dashed black) coverage polygons together with minimum co-pol directivity contours for solid shaped reflector antenna with projected aperture diameter of 3 m (green) and 6 m (blue). The frequency is 3.7 GHz.

An ideal contoured beam consists of a high and uniform antenna gain within the coverage region, no cross-polarization (cx-pol) in this same region and no co-polarization (co-pol) outside of the coverage region, which, however, can only be

achieved under idealized conditions of an infinite aperture size fed by a cx-pol-free feed. The aperture is typically discussed in terms of its electrical size D/λ , where D is the physical diameter of the (projected) aperture, and where λ is the wavelength at the frequency of operation. With reflector antenna size being, on practical grounds, limited to $D \lesssim 3$ m for space applications [1], [2], the electrical size of shaped reflectors may in particular be a limiting factor in lower frequency bands, such as from L to C band [1]. Emerging technologies for realizing very large and deployable apertures include mesh reflectors [3], [4] and faceted reflectarrays [1] that upon further technical maturation may compete with and replace conventional shaped reflector antennas in certain scenarios.

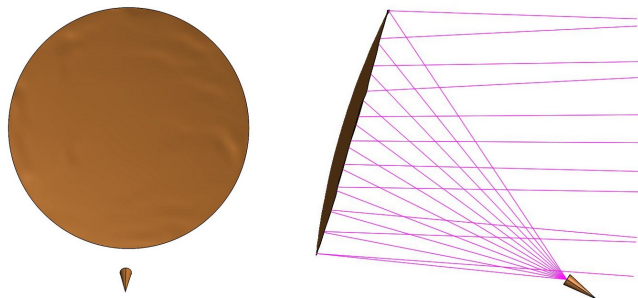


Fig. 2. 6 m solid shaped reflector antenna.

Here, we report a contoured beam RF benchmark study in C band of the conventional solid shaped reflectors, mesh reflectors and reflectarray antennas. As references, we consider the feasible $D = 3$ m and the practically unfeasible $D = 6$ m solid shaped reflectors, and we compare the RF performance of 6 m mesh reflectors as well as of planar and faceted reflectarray antennas with these references. We also compare characteristics and limitations of the emerging technologies.

The paper is organized as follows: In Section II, we introduce the specific coverage and mission requirements, and in Section III the antenna configuration and feed are presented. In Section IV, we describe the RF analysis and results for each of the antenna concepts, and in Section V these results and concepts are discussed. Section VI concludes the paper.

II. MISSION AND COVERAGE

We consider a European coverage as shown by the dashed magenta polygon in Fig. 1. We focus on C band and limit

ourselves to one part of this band from 3.7 GHz to 4.2 GHz, corresponding to a relative bandwidth of 13%, and we consider circular polarization. As design goals, we aim to have a minimum co-pol directivity inside the coverage region of 32 dBi as well as cx-pol discrimination (XPD) of at least 30 dB. Additionally, in France and Germany we require an additional 2 dB of minimum co-pol directivity, that is, a minimum of 34 dBi inside the dashed black polygon in Fig. 1. These requirements are summarized in the second line in Table I.

III. ANTENNA CONFIGURATION AND FEED

We investigate single-offset reflector configurations, and as references we consider solid shaped reflectors with projected aperture diameters of $D = 3$ m and 6 m. In both cases, we fix the focal length to diameter ratio to $f/D = 1$, while the clearance to diameter ratio is $D'/D = 0.1$. The 6 m antenna configuration is shown in Fig. 2.

We use a wizard design in the CHAMP software [5] to set up a corrugated feed horn with 46 corrugations, of which 16 constitute a mode converter. The input (aperture) radius is 36.31 (161.99) mm, and part of the horn can be seen in the inset in Fig. 3. The pattern from this feed is shown in the figure, where solid (dashed) curves are the RHC (LHC) component, and where black (red) [blue] is at 3.70 (3.95) [4.20] GHz. The thin, vertical line indicates the position of the reflector edge. We notice that the part of the cx-pol (LHC) far field illuminating the antenna increases with frequency.

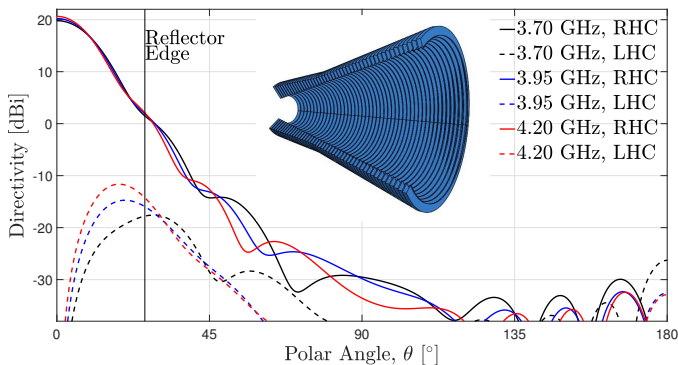


Fig. 3. Pattern from corrugated feed horn, part of which is shown in inset.

IV. RF ANALYSIS AND RESULTS

In Table I, we collect the RF performance of the considered antennas. The second column in the table introduces a shorthand ID for each antenna that we use in the following sections. For the full coverage (dashed magenta polygon in Fig. 1), the minimum co-pol directivity and the minimum XPD at the three design frequencies are presented, while for Germany and France (dashed black polygon in Fig. 1) the minimum co-pol directivity is given. The last column in the table reports the maximum residual, defined as the maximum difference between the goals and the achieved values. In the following subsections, we present and discuss the results for each of the antenna concepts in more detail.

A. Solid shaped reflector antennas

In Fig. 2, we display the 6 m solid shaped reflector antenna. It has been optimized using the POS software [6] and a total of 32×32 splines for describing the surface shaping (1,024 optimization variables, no surface curvature constraints applied). In Fig. 1, we display coverage polygons together with minimum co-pol directivity contours for the 3 m (green) and 6 m (blue) solid shaped reflector antenna at 3.7 GHz. The minimum radius of curvature for the 3 m (6 m) solid shaped surface is 0.06 m (0.39 m).

From Table I, we notice that the minimum directivity contour is about 1.35 dB larger for s6 than for s3. As can also be seen, s3 is not compliant with the mission requirements, whereas s6 is compliant with a margin of 0.57 dB. While $\min(\text{Co-pol})$, for both antennas and in both coverage areas, is relatively constant with frequency, $\min(\text{XPD})$ is substantially lower at the highest frequency than at the lowest one. We ascribe this difference to the relatively different cx-pol feed fields as the frequency is varied, see Fig. 3.

B. Mesh reflector antennas

The mesh reflector antennas are set up based on the 6 m solid shaped reflector. We use that surface and introduce an (x, y) grid in the projected aperture of the shaped reflector (left panel in Fig. 2), and once these nodes, whose z coordinates lie exactly on the shaped surface, have been defined, they are connected by planar triangles. This triangulation thus introduces a surface error compared to the solid shaped one. We stress that for a given solid shaped surface and for a given choice of the mesh reflector node positions, the shaped mesh reflector is fully specified, and there is no additional optimization; one analysis using the GRASP software [7] yields the associated RF performance.

We use a uniform hexagonal grid with a side length of s , s being a parameter. The smaller the value of s , the more nodes and the smaller the surface error, but at the same time the mesh reflector becomes mechanically more complex [8]. With $s = 0.2$ m ($= 0.4$ m), the associated mesh reflector surface is shown in the left (right) panel of Fig. 4, consisting of 821 (199) nodes inside of the reflector rim.

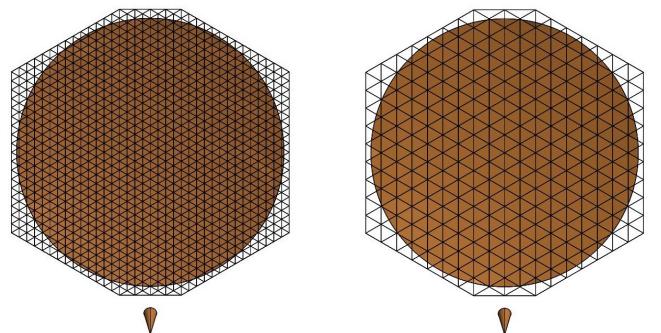


Fig. 4. 6 m mesh reflector antennas with mesh triangle side length $s = 0.2$ m ($= 0.4$ m) in the left (right) panel. Nodes outside of the reflector rim are shown in the GUI in the GRASP software, but play no role in the RF analysis.

TABLE I
MINIMUM CO-POL DIRECTIVITY AND MINIMUM XPD IN FULL COVERAGE AREA AND MINIMUM CO-POL DIRECTIVITY IN GERMANY AND FRANCE AT THREE C-BAND FREQUENCIES AND FOR DIFFERENT TYPES OF ANTENNAS. THE LAST COLUMN CONTAINS THE MAXIMUM RESIDUAL.

Coverage				Full						Germany and France			
Goal				min(Co-pol) = 32 dBi			min(XPD) = 30 dB			min(Co-pol) = 34 dBi			
Frequency [GHz]				3.70	3.95	4.20	3.70	3.95	4.20	3.70	3.95	4.20	
Diameter	ID	Type	Parameter									Res.	
3 m	s3	Solid	–	31.29	31.35	31.29	35.85	32.24	29.25	33.30	33.71	33.99	0.75
	s6		–	32.65	32.70	32.65	34.62	32.05	30.57	34.65	34.74	34.75	-0.57
	m0.1	Mesh	$s = 0.1 \text{ m} (= 1.23\lambda)^a$	32.64	32.68	32.56	34.60	31.96	30.35	34.67	34.78	34.80	-0.35
	m0.2		$s = 0.2 \text{ m} (= 2.47\lambda)^a$	32.43	32.57	32.27	34.59	31.78	29.67	34.69	34.88	34.93	0.33
	m0.3		$s = 0.3 \text{ m} (= 3.70\lambda)^a$	32.14	32.29	31.87	34.19	31.64	28.84	34.66	34.94	35.05	1.16
m0.4	$s = 0.4 \text{ m} (= 4.94\lambda)^a$	31.49	31.38	30.82	35.07	31.50	27.19	34.61	34.84	35.02	2.81		
6 m	pRA1	Planar RA	$L_{ini} = (21, 13.5) \text{ mm}$	31.91	31.91	31.91	29.81	29.81	29.81	33.91	33.91	33.91	0.19
	pRA2		$L_{ini} = (26, 13.5) \text{ mm}$	31.71	31.71	31.71	29.61	29.61	29.61	33.71	33.71	33.71	0.39
	pRA3		$L_{ini} = (21, 11) \text{ mm}$	31.95	31.95	31.95	29.85	29.85	29.85	33.95	33.95	33.95	0.15
	fRA5	Facet RA	tilt = 5°	32.27	32.26	32.25	30.14	30.14	30.14	34.27	34.27	34.27	-0.14
	fRA6		tilt = 6°	32.32	32.31	32.31	30.20	30.21	30.18	34.33	34.32	34.32	-0.18
	fRA7		tilt = 7°	32.26	32.26	32.24	30.11	30.13	30.11	34.26	34.29	34.25	-0.11
	fRA9		tilt = 9°	32.29	32.32	32.25	30.16	30.10	30.07	34.30	34.30	34.29	-0.07
	fRAv		var. $\langle \text{tilt} \rangle = 6.125^\circ$	32.41	32.41	32.40	30.28	30.26	30.26	34.41	34.40	34.41	-0.26

^a λ is the wavelength at 3.70 GHz.

In Table I, we collect the RF performance at four values of s . At the smallest of these (m0.1), min(Co-pol) in the full coverage area is degraded by less than 0.1 dB compared to s6, while the min(XPD) degradation is up to 0.22 dB. In Germany and France, min(Co-pol) increases slightly. Importantly, m0.1 is mission compliant with a margin of 0.35 dB. As s is increased, min(Co-pol) and min(XPD) decrease further in the full coverage area, and m0.2 is not compliant due to the min(XPD) value at 4.20 GHz. Peculiarly, min(Co-pol) in Germany and France continues to increase slightly as s is increased. An important aspect is also the comparison with s3, and both m0.2 and m0.3 in general perform better than s3, though the maximum residual is larger for m0.3 than for s3 due to the relatively low min(XPD) at 4.20 GHz. Finally, m0.4 is comparable in performance to s3 in terms of min(Co-pol), but substantially worse in min(XPD), largely due to the low value at 4.20 GHz.

In Fig. 5, black crosses are mesh reflector degradations of min(Co-pol) in the full European coverage, calculated as the value of the 6 m solid shaped reflector minus that of the mesh reflector, as function of mesh triangle side length, s/λ . As expected, this degradation increases with s , and the blue curve is a second-order polynomial fit that a simple surface error \propto triangle area would predict. This kind of dependence on the triangle side length elucidates the importance of realizing the smallest triangles mechanically possible. A systematic study of the effect of random surface distortions on contoured beam antennas was presented in [9], while, to the best of our knowledge, systematic studies of the effect of regular surface distortions on such antennas have not been reported.

Finally, it is noted that no surface curvature constraints have been used in the optimization of the solid shaped reflector, and thus the penalty of the triangulation is at its maximum. Introducing surface curvature constraints could possibly generate a shaped surface with the same electrical performance, but

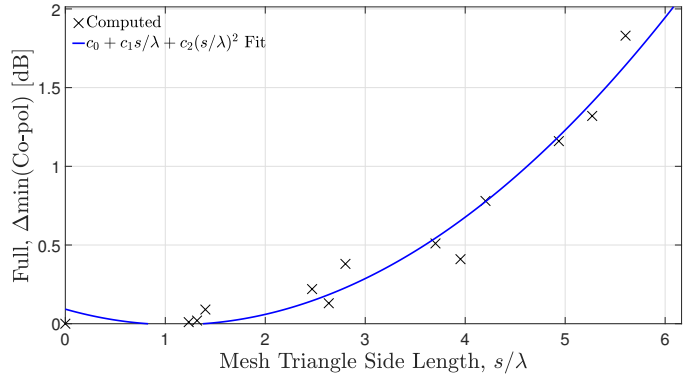


Fig. 5. Mesh reflector degradation of min(Co-pol) in the full European coverage, calculated as the value of the 6 m solid shaped reflector minus that of the mesh reflector, as function of mesh triangle side length, s/λ . Crosses are the computed values, while the blue curve is a second-order polynomial fit.

easier to implement in mesh technology, which could render the $s = 0.2 \text{ m}$ mesh reflector compliant.

C. Planar and faceted reflectarray antennas

We consider a planar and a faceted reflectarray and in both cases optimize the design of square loop-patch elements distributed across the reflectarray surfaces. The element, embedded centrally in a unit cell of $40 \text{ mm} \times 40 \text{ mm}$, is illustrated in the top of Fig. 6, and the loop length, L_1 , and patch length, L_2 , are optimized; the loop width is fixed to $w = 3 \text{ mm}$. The elements are positioned on a substrate of thickness 12 mm and with dielectric constant $\epsilon_r = 1.05$ and loss tangent $\tan(\delta) = 0.0004$. We remark that w could have been included as optimization variable and that, as we return to in Section V, other reflectarray elements could be considered.

The faceted reflectarray consists of nine planar panels, of which the eight non-central ones can be tilted, with four independent tilt axes indicated by colored lines in the bottom

left of Fig. 6. A special case is with all four tilt angles equal to zero, which is the planar reflectarray. By considering finite tilt angles, the faceted surface can be adjusted to approximate the curvature of the solid shaped surface. In the bottom part of Fig. 6, a configuration with an average tilt angle of $\langle \text{tilt} \rangle = 6.125^\circ$ is displayed, and inspection of the antenna from the side (bottom right) reveals its “curved” shape.

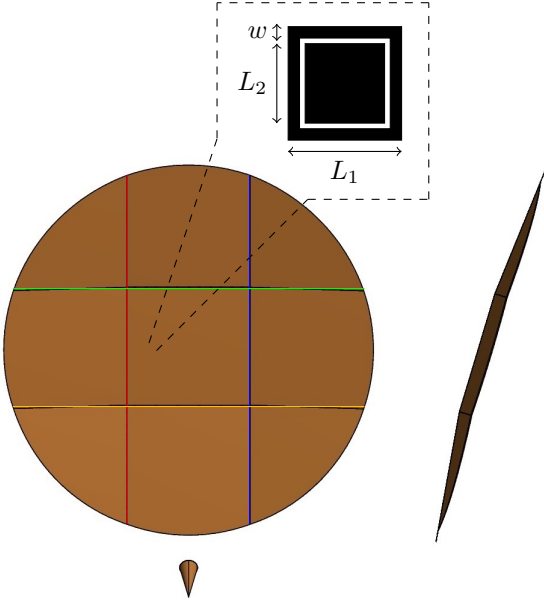


Fig. 6. Faceted reflectarray consisting of nine planar panels, of which the eight non-central ones can be tilted, with four independent tilt axes indicated by colored lines (bottom left). For a specific choice of tilt angles [with tilt angles $(t_b, t_l, t_r, t_t) = (6.5^\circ, 6.0^\circ, 6.5^\circ, 5.5^\circ)$], the antenna is shown from the side (bottom right). Square loop-patch elements, with dimensions as indicated (top), are distributed across the reflectarray surface.

For both types of reflectarrays, the unit cells are packed densely across the surface, and a total of 18,148 loop-patch elements are included and optimized (36,296 optimization variables). For the planar reflectarray, we start the optimization with a uniform distribution of element sizes across the reflector. For the faceted reflectarray, an initial uniform distribution may be sub-optimal due to reflections from the facets, and instead a non-uniform size distribution, determined from a (fast) phase-only optimization, is used. Additional details about the loop-patch element and optimization of the reflectarrays can be found in [10].

For the planar reflectarray, the initial size of the loop-patch element is thus a parameter, and we have investigated three initial sizes, as summarized in Table I (where L_{ini} is the initial values of (L_1, L_2)). We observe a slight variation of the optimized reflectarray performance with this initial size, where pRA3 is marginally better than pRA1. More importantly, none of these planar reflectarray antennas are compliant with the mission requirements, while they in terms of min(Co-pol) perform better than s3, but not in terms of min(XPD).

For the faceted reflectarray, the tilt of the non-central panels is a parameter, and we have investigated different choices for

the tilt, see Table I. For the configurations fRA m , the tilt is identical on all tilt axes (with tilt = m°), while for fRA v there is a variable tilt on each axis (see the caption of Fig. 6). All choices of tilt angles produce reflectarray antennas that are compliant with the requirements, and the choice of tilt has a small effect on the margin. The variable choice of tilt (fRA v), that we have chosen for the faceted surface to be as close to the s6 surface as possible, leads to the largest margin of 0.26 dB. Part of the distribution of loop-patch elements (in the center of the array) in the optimized fRA v configuration is displayed in Fig. 7.

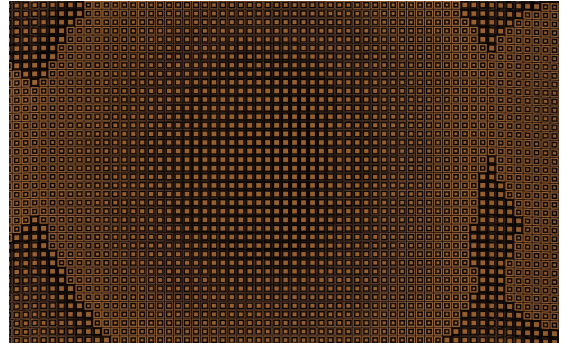


Fig. 7. Part of distribution of loop-patch elements (in the center of the array) in the optimized fRA v configuration.

V. DISCUSSION

The last column in Table I summarizes the maximum residual for each of the investigated antenna configurations, where negative (positive) values correspond to compliant (non-compliant) antennas. These same values are displayed visually in Fig. 8.

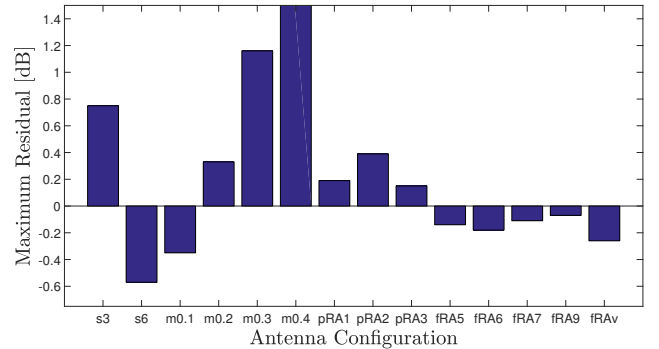


Fig. 8. Maximum residual for antenna configurations. Negative (positive) values correspond to compliant (non-compliant) antennas. The y -axis has been truncated, implying that the value of m0.4 is not shown.

It is apparent that all considered reflectarray configurations, both planar and faceted, perform better than s3, even though the planar ones are not mission compliant. For the mesh reflectors, the performance depends strongly on the triangle side length, with m0.1 and m0.2 (m0.3 and m0.4) performing better (worse) than s3. Among all reflectarray and mesh configurations, m0.1 performs best, being (in terms of maximum

residual) approximately 0.1 dB better than fRAV and 0.2 dB worse than s6.

Inspection of the numbers in Table I reveals that for the solid shaped antennas, and as a consequence for the mesh reflector antennas as well, the residual at the individual goals and frequencies in some cases vary appreciably, while they for the reflectarray antennas essentially remain constant. For s6 at 3.70 GHz, for example, the min(Co-pol) residual is -0.65 dB, but -4.62 dB for min(XPD), while for fRAV these same residuals are -0.41 dB and -0.28 dB, respectively. We attribute this to the larger number of degrees of freedom in reflectarray ($\sim 36,000$) than in solid shaped ($\sim 1,000$) optimizations, which makes it easier to even out the residual across goals and frequencies. This is particularly pronounced for the solid shaped and mesh values of min(XPD) that depend strongly on frequency, which is a direct consequence of the frequency variation of the feed pattern (Fig. 3); this cannot be compensated by the relatively low number of degrees of freedom in these cases.

To shed light on this, we have run an additional s6 optimization (called s6_{MF}) with a modified feed that produces a lower cx-pol far field at all three frequencies. The minimum residual for s6_{MF} is -0.85 dB, and the minimum value of min(XPD) is 35.39 dB (the similar value for s6 is 30.57 dB). That is, in this case min(XPD) is not the limiting factor in terms of compliance, neither for the solid shaped, nor for the mesh reflector antennas that could be derived from s6_{MF}. With this modified feed, the reflectarray performance would also improve, so this investigation does not change the picture of the relative performance between solid shaped, mesh reflector and reflectarray antennas. But it does emphasize that solid shaped and mesh reflector antennas are more strongly dependent on the feed characteristics.

In practice, a mesh reflector with uniformly distributed nodes across the entire aperture (see Fig. 4) cannot be realized, as a mechanical equilibrium of forces in the mesh is required, which gives rise to a slightly perturbed distribution of nodes. It is outside the scope of the present paper to perform a detailed analysis of this question, but it is our experience that this equilibration perturbs the nodes close to the reflector edge, while the nodes more centrally in the aperture remain uniformly distributed [11]. Therefore, with the $s = 0.1$ configuration, we have introduced a random uniform perturbation of the xy -nodes with an amplitude of $\delta = s/2$ for the nodes within a distance of 10% of the radius ($r = D/2$, distance $d = r/10$) from the reflector edge. Analysis of this antenna shows that min(Co-pol) and min(XPD) are degraded by 0.03 dB or less, that is, the effect of mechanical equilibration, within this crude model, is negligible.

Finally, we mention that we have limited the analysis presented in this paper to one part of the C-band (transmit band from 3.7 GHz to 4.2 GHz), while a practical scenario would require a single antenna to work in this as well as in the receive band (from 5.85 GHz to 6.425 GHz). The performance of all considered antennas, both solid, mesh and reflectarray, would be degraded if we were to include requirements in

the receive band. But the most important limitation would be for the reflectarrays, where the limited bandwidth stems from the considered loop-patch element (top of Fig. 6). This element has previously been used in a transmit and receive band design in Ku-band with a bandwidth of 20% [10], but the required 53% bandwidth to cover the full C-band is not feasible with this element; dual-band elements would need to be considered. A previous study from Thales Alenia Space on faceted reflectarrays in C-band was similarly limited to the transmit band [1].

VI. CONCLUSION

We have reported an RF benchmark study between large solid shaped reflector (3 m and 6 m), mesh reflector (6 m) and reflectarray (6 m) antennas for a contoured beam mission in C band. We have in detail described the RF analysis of each of these antenna concepts, and for the mesh reflectors and reflectarrays we have studied associated RF results as function of geometrical parameters that define these antennas. For the mesh reflectors, we have found a strong dependence of the maximum residual in the coverage area with the triangular mesh side length, while for the reflectarrays the maximum residual only depends weakly on the initial element size (planar) and on facet tilt angles (faceted). Finally, several of the considered 6 m mesh reflector and reflectarray antennas perform superior to a conventional 3 m solid shaped reflector, which may pave the way for these antenna concepts in future contoured beam applications, when large (>3 m) apertures are required.

REFERENCES

- [1] R. Chiniard, L. Schreider, N. Girault, S. Vezain, E. Labiote, G. Caille, Y. Baudasse, H. Legay, and D. Bresciani, "Study of a very large reflectarray antenna built with unfoldable panels for missions from L to C band," *CEAS Space Journal*, vol. 5, no. 3, pp. 233–242, Dec 2013.
- [2] D. Alexander, P. Henderson, and G. Turner, "Advancements in large mesh reflector technology for multi-beam antenna applications," in *The 8th European Conference on Antennas and Propagation (EuCAP 2014)*, April 2014, pp. 410–412.
- [3] Y. Demers, A. Liang, E. Amyotte, E. Keay, and G. Marks, "Very large reflectors for multibeam antenna missions," Technical Paper from Northrop Grumman, 2009.
- [4] L. Datashvili, N. Maghaldadze, G. Reinicke, M. Friemel, S. Endler, T. Sinn, P. Zolla, M. Lori, E. Pfeiffer, J. S. Prowald, and A. Ihle, "The Scalable demonstrator: Increasing the TRL of European large deployable antenna reflectors," in *37th ESA Antenna Workshop*, 2016.
- [5] CHAMP Software, TICRA, Copenhagen, Denmark, www.ticra.com.
- [6] POS Software, TICRA, Copenhagen, Denmark, www.ticra.com.
- [7] GRASP Software, TICRA, Copenhagen, Denmark, www.ticra.com.
- [8] J. R. de Lasson, C. Cappellin, R. Jørgensen, L. Datashvili, and J. C. Angevain, "Advanced techniques for grating lobe reduction for large deployable mesh reflector antennas," in *Antennas and Propagation Society International Symposium*, July 2017.
- [9] K. Pontoppidan and S. B. Sørensen, "Shaped beam antennas - reflector surface tolerance effects," in *3rd ESA Antenna Workshop*, 1993.
- [10] M. Zhou, O. Borries, and E. Jørgensen, "Design and optimization of a single-layer planar transmit-receive contoured beam reflectarray with enhanced performance," *IEEE Trans. Antennas Propag.*, vol. 63, no. 4, pp. 1247–1254, April 2015.
- [11] ESA TRP activity "Advanced Techniques for Mesh Reflector with Improved Radiation Pattern Performance", currently ongoing under ESA contract 4000114940/15/NL/MH.